

Analysis of High Resolution Airborne Magnetic Data of Auchi and its Environs Using Centre for Exploration Targeting Grid Analysis

Olurin Oluwaseun Tolutope

Department of Physics, Federal University of Agriculture Abeokuta, Nigeria

Received February 25, 2022, Accepted October 14, 2022

Abstract

High-resolution airborne magnetic data over Auchi and its environ, have been analysed with a view to delineate the geological lineaments, estimate source parameters within the studied area. The geological lineaments were mapped using horizontal gradient magnitude and analytical amplitude signal method. The total magnetic intensity (TMI) values of Auchi and its environs ranges between -68.52885 nT and 79.85480 nT with clear disposition of different geological zone and distinct anomaly ranges. TMI map reflects the variations in the magnetic field intensity and amplitude, indicating variations in lithology and Basement morphology across the study area. The Centre for exploration targeting porphyry analysis revealed and identifies linear geological structures within the study area contained within the high resolution airborne magnetic data through standard deviation. The output estimates magnetic variations and thereafter, filtered using phase symmetry to separate laterally continuous lines. The resulted lineaments was enhanced (Signal to noise ratio) by suppressing noise and background signals using an amplitude thresholding operator which produced vectorization map. The vectorization analysis revealed the Basement rocks which occupy both the eastern and western parts of the study area covered by cretaceous sandstone.

Keywords: *Aeromagnetic; Basement; Lineament; Magnetic anomalies; Vectorization.*

1. Introduction

Airborne geophysical surveys are exceptionally important aspect of modern geophysics. Compared with ground surveys, airborne surveys allow faster and usually cheaper coverage, of large areas. Geophysical methods implemented on airborne platforms include aeromagnetic and magnetic gradient surveys, airborne electromagnetic surveys, airborne radiometric surveys, airborne gravity and gradiometric surveys and airborne remote sensing methods. At the largest reconnaissance scale, the most common airborne surveys are aeromagnetic surveys. Until the last couple of decades, the other primary application of airborne surveys was in mineral exploration [1]. The early use of potential field methods in petroleum was to map sedimentary basin thickness, but high resolution surveys are used to investigate basement trends and intra-formational structures. High resolution methods are now being applied in the groundwater, environmental, and engineering studies [1-2]. Aeromagnetic data have been widely used in exploration since after the World War II [1,3-4]. Recent improvements in acquisition and processing technology enable better understanding of subsurface structure and define the basin architecture. The aeromagnetic survey is a powerful tool in delineating the regional geology (lithology and structure) of buried basement terrain. The detailed aeromagnetic map is a proven to be very effective in cases where the geology of the study area is clearly known. However, the immediate purpose of magnetic surveys is to detect rocks or minerals possessing magnetic properties, which reveal themselves by causing disturbances or anomalies in the intensity of the earth magnetic field. High Resolution Airborne Magnetic (HRAM) survey is the collection of magnetic data over a large expanse of area by small aircraft and

interpreting the data using several interpretational techniques [6]. HRAM surveys have a resolution in the nanotesla scale such that in addition to adequately mapping magnetic rocks which can be adopted to map intra-sedimentary faults segment with elevated magnetic minerals deposit concentration that generate small variation in the anomalies. The tiny variations in the intensity of the ambient magnetic field due to the effect of temporal constantly varying solar and spatial variations in the earth's magnetic field logged measured by magnetometer as the aircraft flies. This is as a result of both earth regional magnetic field, and the local effect of magnetic minerals in the earth crust. The correction done by subtracting the solar and regional effects, the resulting airborne magnetic map shows the spatial circulation and comparative great quantity of magnetic minerals in the upper levels of the crust [7-9]. The magnetic method has come into use for identifying and locating masses of igneous rocks that have relatively high concentration of magnetic minerals (magnetite). Magnetite is the most common ferromagnetic mineral and in most cases, the magnetic permeability is determined by the amounts of magnetite and related minerals available in the rock which can be measure using magnetic survey. Also, determination of trends, extents and geometries of magnetic bodies in an area, and to interpret them in terms of geology can be accomplished with the help of magnetic survey. Structural trends are faithfully reproduced in magnetic patterns, but assignment of rock type is ambiguous, since ranges of values of magnetic susceptibilities of different rock types may overlap [10-18].

This present work is an attempt to provide better understanding of the structural framework, geological features and the sources parameters which can be an aid to further exploratory efforts in the area under consideration. The processes involves analyzing and interpreting high resolution magnetic data collected with flight spacing of 400 m and elevation of 80 m. This will be achieved using Fourier filtering, gradient enhancement and CET techniques. When interpreting aeromagnetic data, it is necessary to compare structures or magnetic anomalies delineated from the derivatives with the geology of the area under consideration.

2. Geological setting

The Auchi formation is composed mainly of coal measures with rivers flowing through its boundaries. Other minerals within the Auchi region include coarse porphyritic biotite/hornblende-biotite & granodiorite, porphyroblastic gnesis, and undifferentiated older granites mainly porphyritic granite with porphyroblastic gnesis. Other minerals of close proximity to the Auchi region includes fine grained, flaggy, quartz-biotite-schist and gnesis. [19] and [20] indicated that the study area is composed of migmatite-gneiss-quartzite complex with little supra-crustal rock relics. Auchi falls within a region known as the Precambrian basement complex of the country. This is composed of a suite of crystalline rocks which have been exposed in over nearly half of the country. However, [21] in the year 1976 and Ball in the year 1980 mentioned that the basement complex of Nigeria is zoned in the western part of the Pan-African shield. Such region extends west into the Dahomey of Benin Republic [22]. The dominant lithologic units of the study area are gneisses of migmatite, biotite and granite which are regionally emplaced; the ferruginous quartzite is the source of the iron ore mineralization in the area [23]. The lithology of this region of study can be identified from the geologic map of the study area. These materials include quartzite, migmatite, schist with pegmatite intrusion, biotite rich granites, charnokitic rocks, and quartzite and quartz schist, Augen gnesis, calc-gnesis, marble, and metaconglomerate (Figure 1).

3. Material and method

3.1. Data description

The data set (aeromagnetic data) used in this study were magnetic anomaly field (sheet number 266) acquired during high resolution airborne geophysical surveys of Nigeria by Fugro Airborne Survey Limited for Nigerian Geological Survey Agency between year 2003 and 2009 [24]. The survey was flown in drape mode using real time differential Global Positioning System (GPS) at a sensor mean terrain clearance of 75m. Traverse and tie line spacing were 500 m

and 2000 m respectively while flight and tie line directions were NW-SE and NE-SW respectively [24]. The aeromagnetic data were obtained using a proton precession with resolution of 0.1 nT. The flight line direction was in the direction 135 azimuths while the tie line direction was in 45 azimuths. The average magnetic inclination, magnetic declination and magnetic field strength across the survey were 14.02°, 3.83° and 32,446.006 nT respectively. The data were de-cultured, leveled, corrected by removing International Geomagnetic Reference Field 2008 (IGRF), gridded at an appropriate cell size that enhances anomaly details and reduces possible noise and latitude

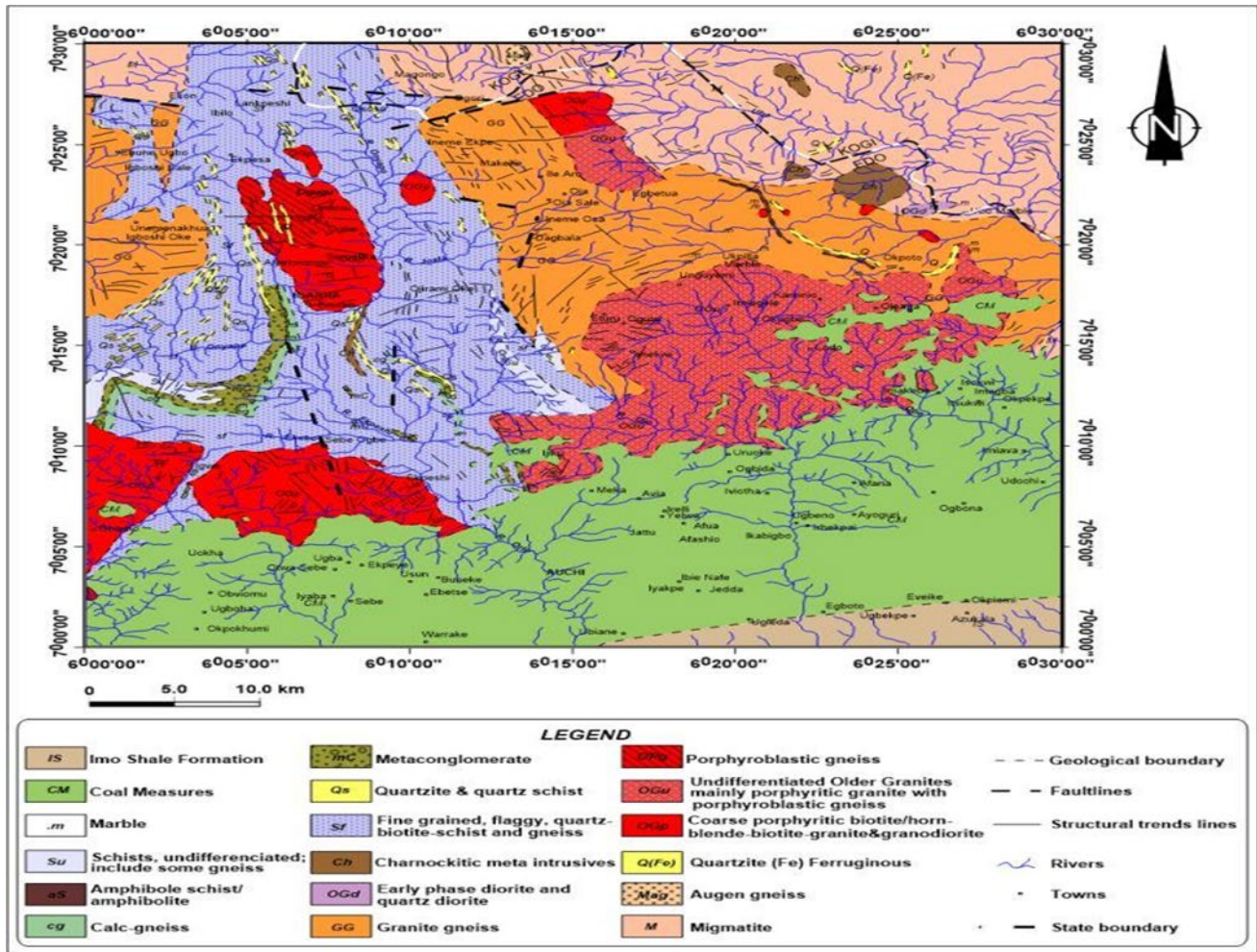


Figure 1. Geological Map of the Auchi and its environs

3.2. Magnetic data processing

The processing of the magnetic anomaly data is based on the analysis of the computer digitized compiled information using minimum curvature gridding techniques at different altitudinal levels (elevation) from measured total magnetic intensity of the study area as shown in Figure 2. This gridding method fits minimum curvature curves to the data point as well as producing visually alluring maps from irregularly spaced data and attempts to express trends suggested in the data using methods described by [25].

3.3. Data filtering

The area under consideration is made up of Basement Complex, thus the interest was to remove cultural effect and enhance short wavelength signal emanating from shallow geologi-

cal features. Digitized aeromagnetic data were made to improve its quality for better understanding of the subsurface geology of the deposit by filtering operation [26-27]. The desired improvements on the quality of the aeromagnetic data was achieved by the application of two dimensional Fast Fourier transform filter i.e. upward continuation, Reduction to equator.

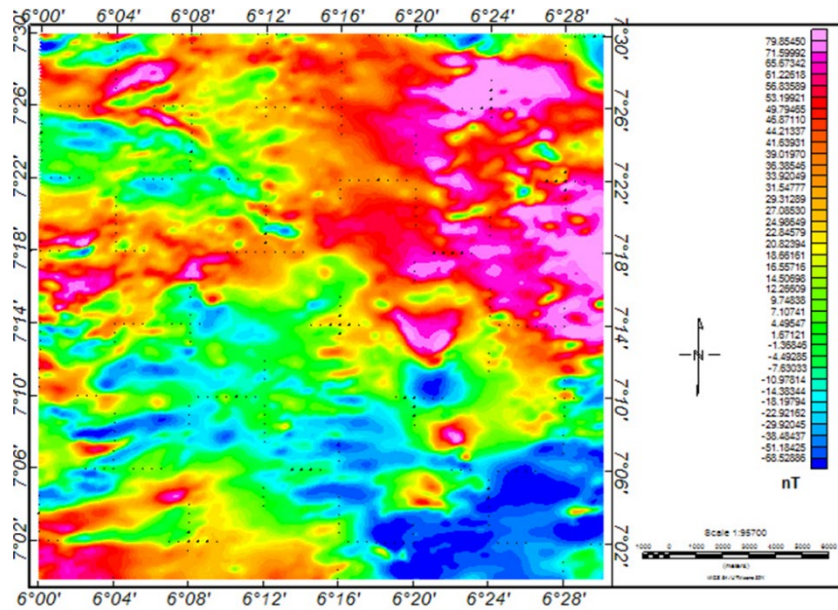


Figure 2. Magnetic Intensity (Magnetization) Map of Auchi and its Environs

4. Interpretational techniques

4.1. Reduction to equator reduction to equator RTE

Auchi and its environs were situated at low magnetic equator and since Earth’s (back-ground) magnetic field intensity decreases from the poles of the equator, thus, the peaks of magnetic anomalies were wrongly positioned over their sources as well as skewed along a particular given direction. Therefore, this makes interpretation magnetic anomalies complex, uncorrected. However, at low magnetic latitude, a special reduction to equator which transforms the observed magnetic anomaly at equator into anomaly that would have been measured if the magnetization and ambient field were both vertical was proposed by [28]. RTE operation transforms theoretical magnetic anomalies located at the pole and magnetized by induction only into the observed magnetic anomalies.

The desired improvements on the quality of the aeromagnetic data were achieved by the application of two dimensional Fast Fourier transform. [28] assumed that set of observed magnetic data acquired on planar observation surface. [28] modify earlier work done by [29], where express reduction to pole operation in wavenumber domain is given as equation 1,

$$A_T(u, v) = \frac{A_o(u, v)}{(\sin I + i \cos I \cos I \cos(D - \theta))^2} \quad (1)$$

where D and I is the declination and inclination of the core field, (v, u) is the wavenumber corresponding to the $\Delta z > 0$ directions respectively, $\theta = \tan^{-1}\left(\frac{u}{v}\right)$ and $i^2 = -1$.

Taking horizontal magnetization into consideration, $I = 0$ and $D - \theta$ is close $\pm 90^\circ$, which makes the imaginary part close to zero, thus reduction to pole processing will be unstable at low latitude and singular at the equator. In order to overcome this complexity, the entire observed magnetic field were subjected to Fast Fourier transform (FFT) given as equation 2

$$A_o(u, v) = A_T(u, v)(\sin I + i \cos I \cos I \cos(D - \theta))^2 \quad (2)$$

According [28] application of inverse Fourier transform to equation 2 gives equation 3;

$$F^{-1}A_o[(u, v)] = [A_T(u, v)(\sin I + i \cos I \cos I \cos(D - \theta))^2] \quad (3)$$

4.2. Upward continuation

Upward continuation filter operation allows the transformation of data measured on one surface to some higher surface [1] and have tendency to smooth the acquired data by attenuating short-wavelength magnetic field anomalies signatures relative to their corresponding long – wavelength. [4] showed the expression for upward continuation from Green’s third identity of a potential field measured on a level $z = z_0$ at the point $P = (x, y, z_0 - \Delta z)$;

$$(x, y, z_0 - \Delta z) = \frac{\Delta z}{2\pi} \int_{-\infty}^{\infty} \int_{-\infty}^{\infty} \frac{U(x', y', z_0)}{[(x-x')^2 + (y-y')^2 + \Delta z^2]^{\frac{3}{2}}} dx' dy', \Delta z > 0 \quad (4)$$

Applying the Fourier convolution to equation 5 gives;

$$F[U_u] = F[U]F[\Psi_u] \quad (5)$$

where $\Psi_u(x, y, \Delta z) = \frac{\Delta z}{2\pi(x^2 + y^2 + \Delta z^2)^{\frac{3}{2}}}$ is the analytical expression of $F[\Psi_u]$ and $F[U_u]$ is the Fourier transform of the upward continuation field.

Thus, the upward continuation filter equation is given by Equation 6

$$F[\Psi_u] = e^{-\Delta z|k|}, \quad \Delta z > 0 \quad (6)$$

4.3. Vertical gradient

Vertical gradient derivative was proposed by [30] by applying Three Dimensional (3D) Hilbert transforms in the x and y directions. The vertical derivatives of the gradient analysis can be applied to potential field data either in frequency or space domain. In this study, vertical gradient derivative was used to enhance shallow subsurface structural features with their boundaries edges and associated lineaments. This technique amplifies short wavelengths of higher frequencies at the expense of longer wavelength anomalies, in order to magnify and mapped shallower causative sources. The algorithm for vertical gradient is given as equation 7 [29];

$$A(u, v) = A(u, v) \left(\frac{(u^2 + v^2)^{\frac{1}{2}}}{n} \right)^n \quad (7)$$

Where $A(u, v)$ the amplitude present at a given frequencies, n is the order of the derivative.

4.4. Analytic signal amplitude

Analytic signal amplitude is a filtering transform formed through the combination of horizontal and vertical gradient of a magnetic anomaly field. Nabighian [7,31] evolved the concept of the transforming analytic signal amplitude for magnetic response and showed that its amplitude gives a bell-shaped function over each corner of a 2D anomaly (body) with polygonal cross-section. The amplitude, A of the analytic signal of the total magnetic field T is calculated from the three orthogonal derivatives of the field using Hilbert transform can therefore be written as Equation 8. This filter applied to reveal the anomaly texture and highlight discontinuities also enhance short- wavelength anomalies [32].

$$|A(x, y, z)| = \left[\left(\frac{dT}{dx} \right)^2 + \left(\frac{dT}{dy} \right)^2 + \left(\frac{dT}{dz} \right)^2 \right]^{1/2} \quad (8)$$

Equation 8, reveals the location of the source in the horizontal plane which can therefore be deduced from the peak position of the amplitude of the analytic signal and the source depth can be estimated as the half width of the half maximum of the amplitude of the analytic signal [32].

4.5. Horizontal gradient magnitude

The horizontal gradient magnitude is the least susceptible to noise in the data and interference effects between nearby sources during the analysis, because it only requires calculation of the first-order horizontal derivatives of the magnetic field. Horizontal gradient magnitude can be therefore be calculated using Equation 9. Mathematical and theoretical details HGM are as discussed by [20, 33-37].

$$HG(x, y) = \sqrt{\left(\frac{dT}{dx} \right)^2 + \left(\frac{dT}{dy} \right)^2 + \left(\frac{dT}{dz} \right)^2} \quad (9)$$

4.6. Pseudo-gravity transformation

In 1957, [38] used Pseudo-gravity transformation to transform magnetic data using Poisson's equation to make easy the interpretation of the magnetic map. The Pseudo-gravity transform enhances the anomalies associated with deep magnetic sources at the expense of the dominating shallow magnetic sources. It is suitable transform for interpreting deep seated mineral plumbing's systems associated with known shallow minerals occurrences [38]. Thus, [38] transforms Poisson's equation using Fourier transform as shown in Equation 10.

$$\mathcal{F}[g_m] = -\frac{\gamma \rho}{c_m M} \mathcal{F}[V] \quad (10)$$

4.7. Centre for exploration targeting grid analysis

Centre for Exploration Targeting (CET) is a matching set of algorithms operation which provides functionalities for enhancement of geological structures, lineament detection and structural complexity analysis of potential field data [39-43]. CET spontaneously delineate lineaments and identify promising areas of foreign deposits (anomaly) through demarcation of convergence regions and divergence of structural geometry using advanced statistical steps which include lineation delineation, texture analysis, vectorisation and complexity analysis to produce occurrence contact density map.

4.8. Centre for exploration targeting porphyry analysis

Centre for Exploration Targeting Porphyry is suite of algorithm that centered a circular feature with their boundaries being zones of weakness that help to ascend hydrothermal solutions. In order to delineate these features associated with them, CET porphyry approach was used to process the RTP data of the studied area. The alteration zone and intrusion itself are generally associated with positive magnetic anomalies signatures. The outer alteration zones are much less magnetic in nature [44].

5. Discussion of results

The magnetic intensity (TMI) values of Auchi and its environs ranges between -68.52885 nT and 79.85480 nT with clear disposition of different geological zone and distinct anomaly ranges. The MI map (Figure 2) reflects the variations in the magnetic field intensity and amplitude, indicating variations in lithology and basement morphology across the study area. The blue portions of the maps represent the minimum magnetic intensity (moderate negative amplitude anomaly) areas; while the red color portions represent the maximum magnetic regions (strong amplitude anomaly). The study area is marked by both high and low magnetic signatures, which could be attributed to several factors such as; variation in depth, difference in magnetic susceptibility, difference in lithology and degree of strike. This enables identification of zones with significant -nT in blue colour are dominated in the SW part and scattered across some parts of the study area while the maximum magnetic intensity are dominated in the NE and scattered in some part of the study area. The long wavelength anomaly signatures within the area under consideration is as a result of the underlying Basement and the short wavelength anomalies signatures are typically due to the presence of magnetized bodies at shallower depths (that is; near surface depth). The high amplitude and prominent long wavelength magnetic responses trending in the E-W in the north-eastern region might be due to a deep-seated rock of relatively low magnetic susceptibility in the area. High amplitude anomalies are noticeable around Magongo, Egbetua, Ugbo, Igboshi oke, Ubo, Eturu Ogute, Okugbe, Igarra and northern part of the map. Ekpesa, Ibilo, Nneme Ekpo Oja sale and Dagbala also displayed relatively high amplitude magnetic intensity response. Imagbon, Igbaga, Imeri. Auchi, Ugoha, Obviomu, Jattu, Uokha, Ekpeye, Avia and Udochi are regions that exhibit low amplitude magnetic signatures. Most of these places coincide with portion of the study area with thin to relatively thick sedimentary cover, where the effect of the thick weakly susceptible clastic materials masks the high magnetic susceptibility emanating from relatively deep basement rocks

The reduction to equator of the magnetic intensity map (Figure 3) reveals the correction in the asymmetries of the observed magnetic anomalies which had been minimized and centres

the anomalies signatures directly over the causative elongated bodies. The reduced to equator magnetic intensity values for the study area ranges from -55.048 nT to 70.082 nT . The reduced to equator map characterized with low frequencies signatures, long wavelengths, weak intensity, sharp low amplitude and nearly irregular-shaped anomalies, which may due to near-surface sources, such as shallow geologic units and cultural features.

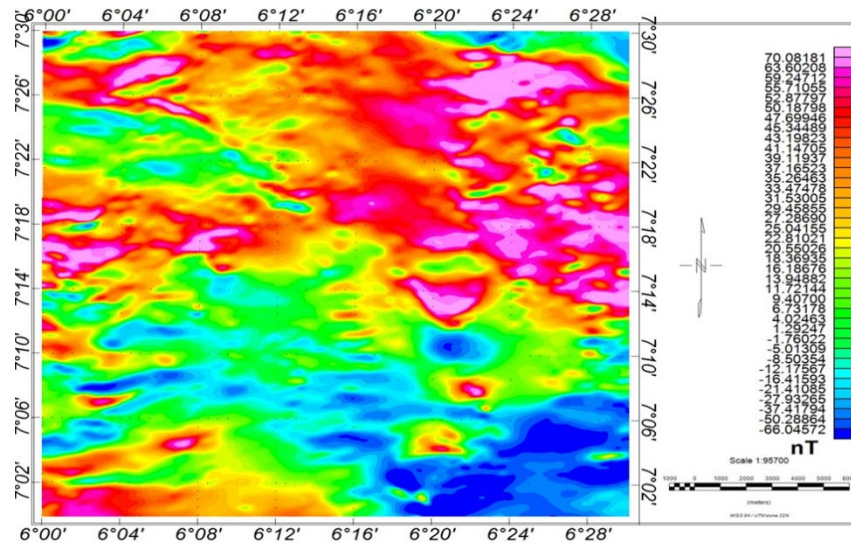


Figure 3. Reduction to equator of the magnetic intensity map

The vertical gradient derivative map revealed near subsurface geological features such as faults as presented in Figure 4 gives a good representation of short wavelength anomalies with high frequency of continuous trend. Vertical gradient operator filter enhances short-wavelength anomalies responsible for shallow sources at the expense of long wavelength. It is obvious that the north-eastern, south-eastern parts of the study area were dominated with clusters of short wavelength anomalies indicating a relatively shallow depth of the causative sources in comparison with the southern part where there are long wavelengths were observed. It can be concluded a deeper sources conformable with the presence of a sedimentary cover. Also, the first vertical derivative map revealed that E – W trend is the most pronounced directions in the area.

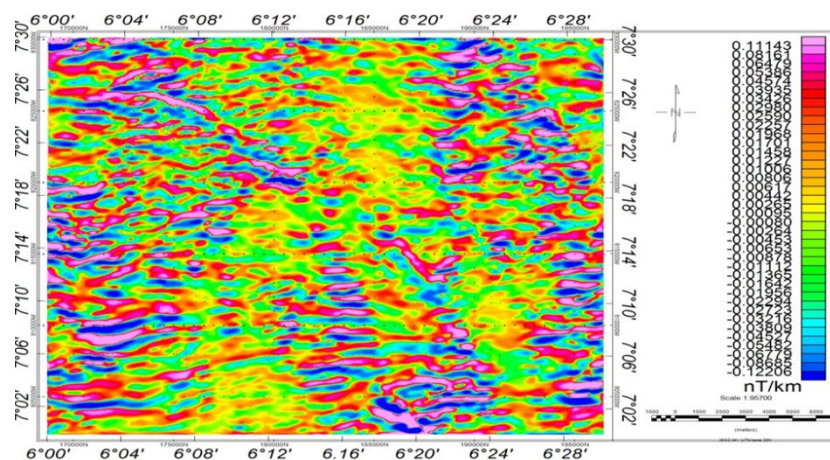


Figure 4. Vertical derivative of magnetization map of Auchi and its environs

The reduced to equator total magnetic intensity data were subjected to Horizontal Gradient Magnitude (HGM) algorithm, which provides an effective exposure of magnetic anomalies lineaments which could be attributed geological structures, such as; folds faults and contact locations. The HGM of the magnetic intensity of the study area ranges from 0.0457 to

0.15247nT with cluster of short wavelength anomalies signatures trending from western to southern part of the study attributed to intrusive bodies and geological structures on the HGM map as presented in Figure 5. The HGM maximum gradient (the black lines on the map) forms linear pattern using CET analysis. Figure 4 show that the structures within the subsurface trend in the E-W, NW-SE, NE-SW, WNW-ESE and ENE-WSW directions.

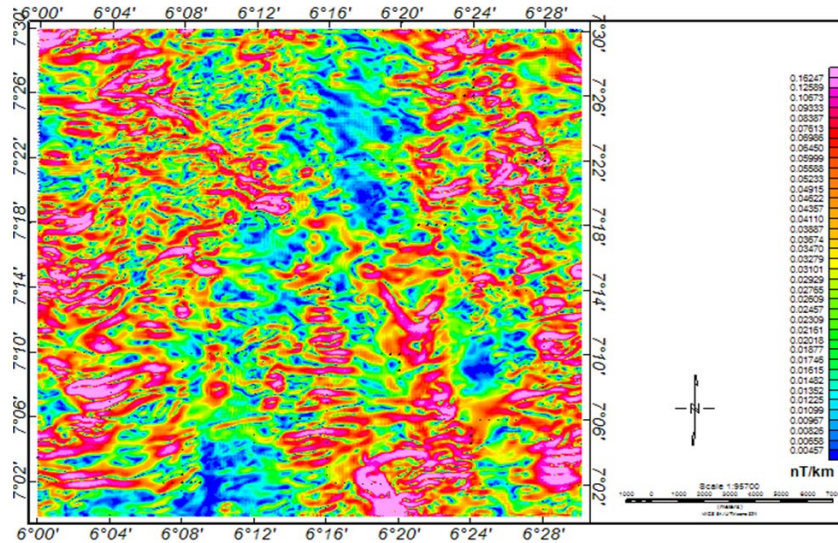


Figure 5. Horizontal gradient magnitude of magnetic intensity of Auchi and its environs

Analytic signal amplitude (ASA) map of Auchi and its environs (Figure 6) was generated from analytic signal amplitude grid computed from combination one vertical gradient and first order vertical derivatives values of reduced to equator total magnetic intensity of the study area.

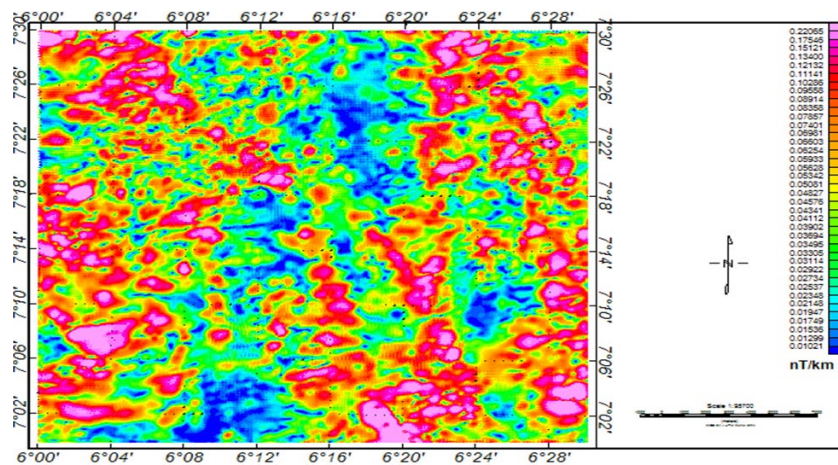


Figure 6. Analytical signal amplitude of Auchi and its environs

ASA map of the study area shows the amplitudes of the magnetic signature highlights discontinuities and anomaly texture. Protruding high amplitude analytic signal anomalies signatures are apparent on the analytic signal map. The analytic function form an envelope of possible phase shift of the observed anomaly and peaks over geological structure (contacts). The analytic signal amplitude map also shows the attenuation of shallow sources features. The magnitude of the amplitude of magnetic gradient intensity ranges from 0.010221 to 0.22055nT/km. Some regions in the map characterized with very high amplitude which reflects lithological variation in magnetic basement, such as; ophiolitic serpentine, ophiolitic metagabbro, gabbroic rocks, dokhan volcanic and hammamat felsite as these rocks have high ferromagnesian with large amount of felsic minerals. The parts of the study area are dominated

with low amplitude and indicates presences of thick sediment covering the weathered Basement. and metasediments.

The Upward Continuation (UC) operation filter was applied to the reduced to equator at low latitude magnetic data of Auchi, south-south Nigeria at various wavelength. The RTE magnetic gridded was upward continued at wavelength of 5m, 10m, 15m and 20m. The UC operator smoothens and filters out response of high frequency noisy data which correspond to near surface effects. The enhanced deeper source and smoothed effects which are contributions from subsurface geological formation having the response of magnetic variation ranges between, -61.8 to 61.7, -63.4 to 59.3nT, -63.1nT – 59.1nT, and - 62.9 – 58.9nT at depths of 5 m, 10m, 15m, 20m and 25m respectively as presented in Figures 7a,7b,7c and 7d. The upward continuation solution also reveals that the variation in magnetic intensity decreases in value with increasing continuation distances. The apparent susceptibility map Figure 8 revealed the apparent susceptibility of the magnetization ranges from -0.00051 to 0.00058 SI. The region of positive magnetic susceptibility could be due to the rock rich in diamagnetic minerals, and are predominantly found around Azuka, Egbota, Eveike, Okpoto, Igboshi oke, and Magongo. Region of intermediate magnetization which are found to be lying over Ibilo, Ankpeshi, Egbetuwa and Ugbo. Region of negative magnetic susceptibilities (low magnetization) were observed around the Udochi, and Ogbona. This low magnetization is as a result of thick sediment around the noted area [45].

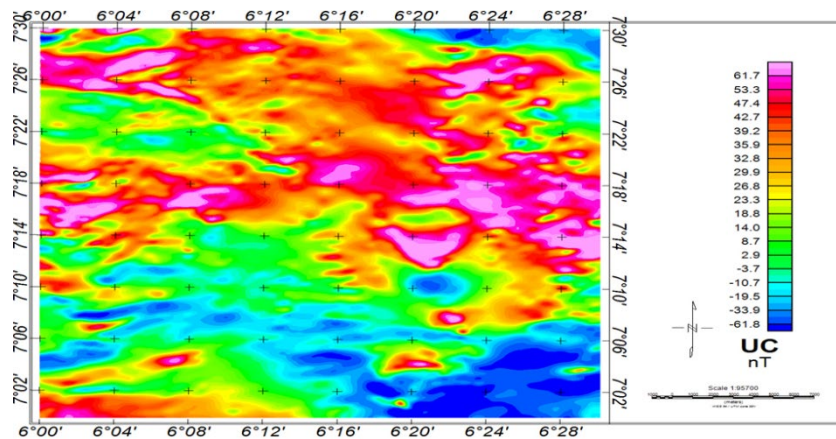


Figure 7a. Upward continuation map Auchi and its environs at Depth 5m

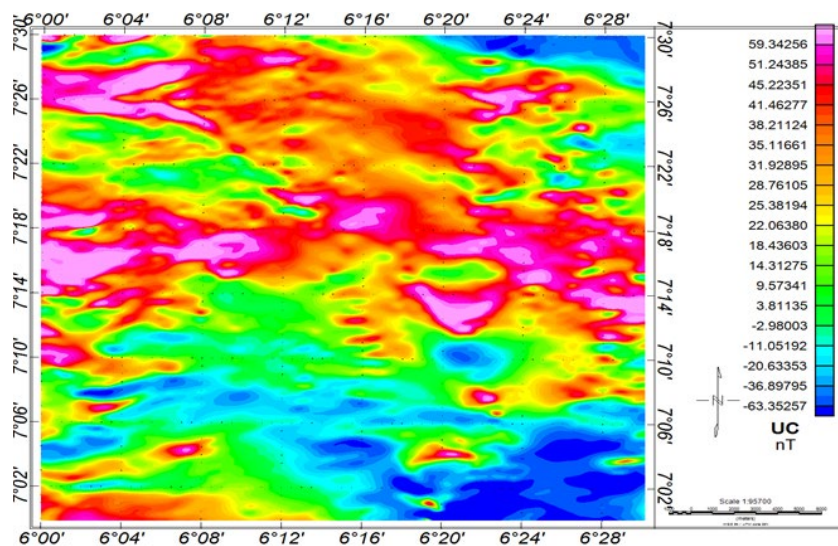


Figure 7b. Upward continuation map Auchi and its environs at Depth 10m

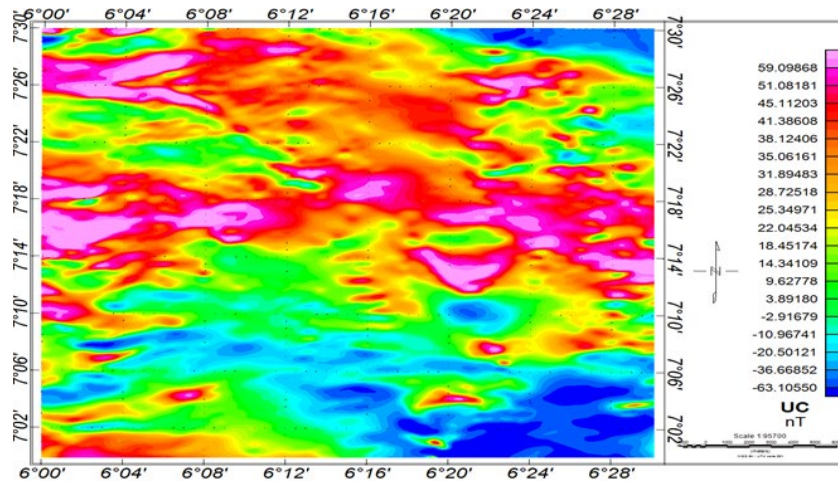


Figure 7c. Upward continuation map Auchi and its environs at Depth 15m

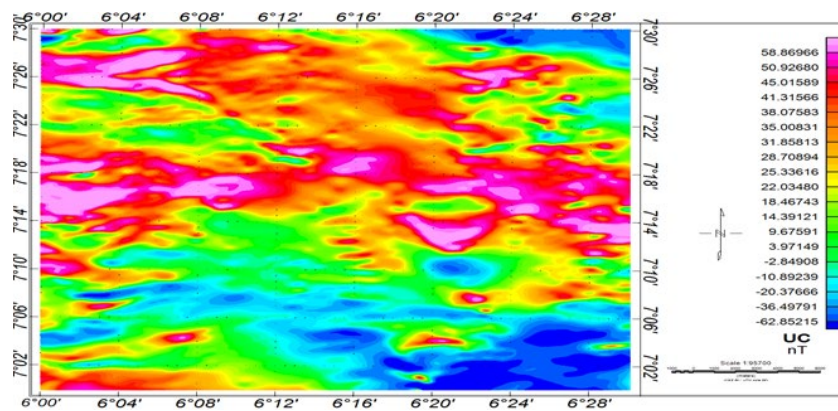


Figure 7d. Upward continuation map Auchi and its environs at Depth 20m

The reduced to equator magnetic grid was also subjected to CET analysis filtering operator. The CET grid was carried out on gridded data which identify linear geological structures contained within the high resolution airborne magnetic data through standard deviation. The output estimates magnetic variations and thereafter, filtered using phase symmetry to separate laterally continuous lines.

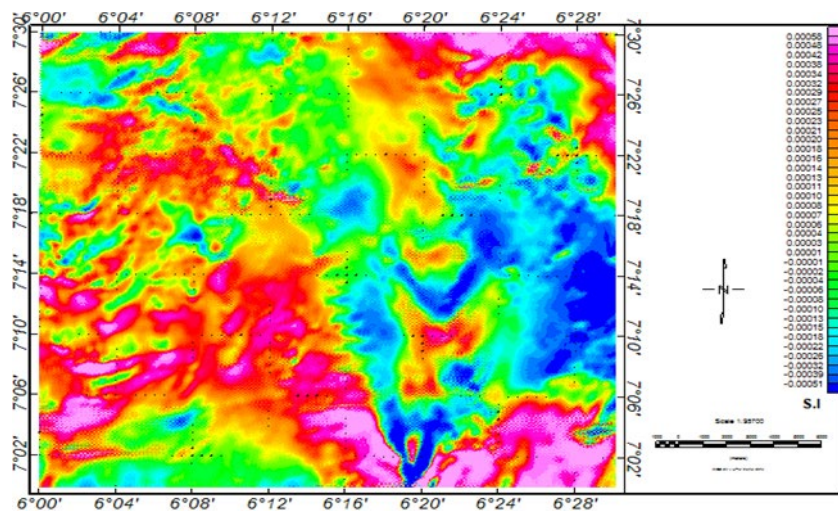


Figure 8. Apparent susceptibility map of Auchi and its environs

The resulted lineaments were enhanced (Signal to noise ratio) by suppressing noise and background signals using an amplitude thresholding operator which produced vectorization map as presented in Figures 9. The vectorization map revealed the basement rocks which occupy both the eastern and western parts of the study area covered by cretaceous sandstone. A large number of faults and shear zone have been identified as presented in Figure 8. In Figure 9, occurrence of contact which is the demarcation between two geological formations was well pronounced in the density heat map, which is based on the automated lineament detection output. The gridded magnetic data was subjected to CET Porphyry algorithm and the output (Figure 10) reveals the orientation for minerals deposition and showing a high probability for further mineral deposition in the study area.

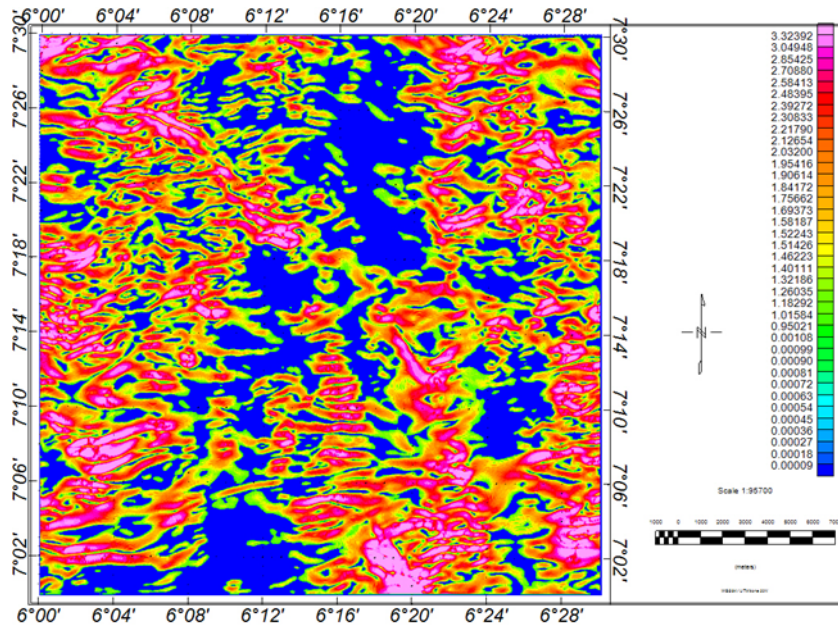


Figure 9. Entropy /Lineament of Auchi and its environs

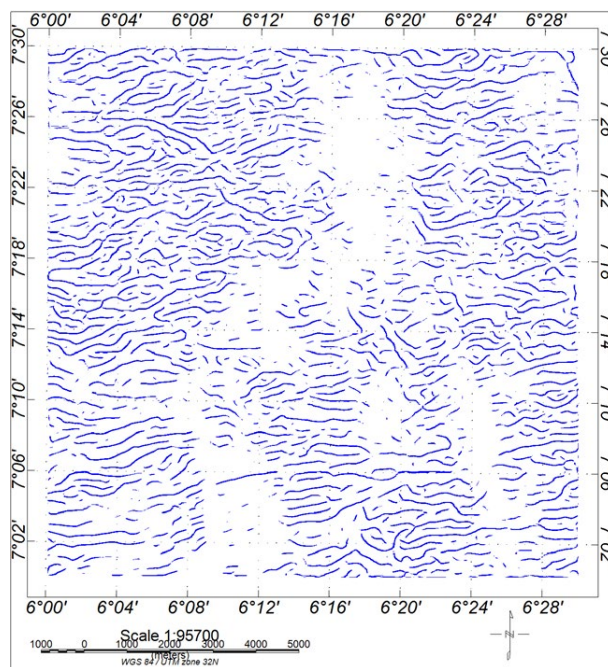


Figure 10. CET porphyry lineament trend of Auchi and its environs

6. Conclusion

Interpretation of the high resolution airborne magnetic data sets revealed the both geological parameters and geological structure within the study area. The Reduction to Equator of magnetic map of Auchi and its environs revealed series of parallel continuous linear features taken NW, SW, E-W trends with variable signature of magnetic amplitudes, which are related to dyke, faults and shear zones. Also, RTE magnetic map showed strong positive and negative magnetic anomalies signatures generating contact zones (demarcation), which may be considered with the linear geological features as prospective zones for mineralization. Analytic Signal Amplitude analysis produced ASA map that clearly categorize the granite gneiss, porphyroblastic gneiss and coarse porphyritic from the surrounding rocks of the southwest Nigeria Basement Complex based on geological geometry. ASA map of the study area also reveals the amplitudes of the magnetic signatures which highlights discontinuities and anomaly texture. Protruding high amplitude analytic signal anomalies signatures are apparent on the analytic signal map. The results of CET Grid analysis and CET porphyry reveals structural complexities, porphyry (dyke-like structures) and known mineralization prospects zone.

References

- [1] Nabighian MN, Philip JD, Granch VJS, Hansen RO, and Pierce JW. The historical development of the magnetic method in exploration. *Geophysics*, 2005; 70: 28–32.
- [2] Grauch VJS, Phillips JD, Koning DJ, Johnson PS, and Bankey V. Geophysical interpretation of Southern Espanola Basin, New Mexico, USGS Professional paper, 2005; 1761, 88
- [3] McIntyre JI. Geologic significance of magnetic patterns related to magnetic in the sediments and meta-sediment. *Bulleting of Australian society of exploration. Geophysics*, 2005; 11:19 – 32.
- [4] Blakely RJ. *Potential theory in gravity and magnetic applications*: Cambridge University Press. 1995
- [5] Reeves C. *Aeromagnetic Surveys: principle, practice and interpretation*. Geosoft INC, 2005; 155 p.
- [6] Hsu KS, Coppens D, Shyu CT. Depth to magnetic source using the generalized analytical signal. *Geophysics*, 2002; 63: 1954 – 1957
- [7] Nabighian MN. The Analytic signal of two dimensional bodies with polygonal cross section-its properties and use for automated anomaly interpretation. *Geophysics*, 1972; 37: 507-517.
- [8] Bhattacharyya BK. Energy density spectrum and autocorrelation function of anomalies due to simple models. *Geophysical prospecting*, 1966; 14: 242 – 272.
- [9] Spector A and Grant F. Statistical models for interpreting aeromagnetic data: *Geophysics*, 1970; 35, 293–302.
- [10] Damaceno JG, de Castro DL, Mocitaiba LSR. Geophysical study of volcanic bodies, Potiguar Basin (RN): preliminary results. In: 14th International Congress of the Brazilian Geophysical Society Rio de Janeiro Brazil August 3-6 2015: 1-4.
- [11] Costanzo-Alvarez, V, Aldana M, Aristeguieta O, Marcano MC and Aconcha E. Study of magnetic contrasts in the Guafita oil field (South-western Venezuela). *Physics and Chemistry of the Earth, Part A: Solid Earth and Geodesy*, 2000; 25(5): 437- 445.
- [12] Kearey P and Brooks M. *An Introduction to Geophysical Exploration*. 3rd Edition. Blackwell Science Publication, 2002
- [13] Aldana M, Costanzo-Alvarez V and Diaz M. Magnetic and mineralogical studies to 367 characterize oil reservoirs in Venezuela. *The Leading Edge*, 2003; 22(6): 526
- [14] Ghazala HH. Geological and structural interpretation of air borne surveys and its significance for mineralization, southeastern desert Egypt. *Journal of African Earth Sciences (and the Middle East)*, 1993; 16(3): 273-285
- [15] Chernicoff CJ, Richards JP and Zappettini EO. Crustal lineament control on magmatism and mineralization in northwestern Argentina: Geological, geophysical and remote sensing evidence. *Ore geology reviews*, 2002; 21(3-4): 127-155
- [16] Porwal A, Carranza EJM and Hale M. Tectonostratigraphy and base-metal mineralization controls, Aravalli province (Western India): New interpretations from geophysical data analysis. *Ore geology reviews*, 2006; 29(3-4): 287-306

- [17] Allek K and Hamoudi M. Regional-scale aeromagnetic survey of the south-west of Algeria: A tool for area selection for diamond exploration. *Journal of African Earth Sciences*, 2008; 50: 67-78
- [18] Schetselaar EM and Ryan JJ. Remote predictive mapping of the Boothia mainland 527 area, Nunavut, Canada: an iterative approach using landsat ETM, aeromagnetic and 528 geological field data. *Canadian Journal of Remote Sensing*, 2009; 35: S72-S94
- [19] Oversby VN. Lead isotope study of Aplites the precambian basement rocks near Ibadan, southwestern Nigeria. *Earth and Planetary Science Letters*, 1975; 27: 177-180
- [20] Olarewaju VO. Geochemistry of the charnockitic and granitic rocks of the basement complex around Ado-Ekiti, southwestern Nigeria. Ph.D. Thesis, University of London, U. K, 1981
- [21] McMurry P. The Geology of the Precambrian to Lower Paleozoic Rocks of Northern Nigeria - A Review, in C.A. Kogbe (ed.), *Geology of Nigeria*, Elizabethan Press, Lagos, 1976; p. 15-39
- [22] Amigun JO and Ako BD. Rock density- A tool for mineral prospecting: A case study of Ajab-anoko iron ore deposit, Okene SW Nigeria. *The pacific journal of science and technology*, 2009; 10: 733-744.
- [23] Olade MA. Evolution of Nigeria's Benue Trough. *African Lithosphere and their Geodynamic Significance. Journal of African Earth Science*, 1975; 3: 437 - 442.
- [24] Nigeria Geological Survey Agency. 2009
- [25] Briggs I. Machine contouring using minimum curvature. *Geophysics*, 1974; 39:39-48
- [26] Hildenbrand APY, Gillot V, Soler and Lahitte P. Evidence for a persistent uplifting of La Palma (Canary Islands), inferred from morphological and radiometric data, *Earth Planet. Sci. Lett.*, 2003; 210(1-2), 277-289
- [27] Hinze WJ, von Frese RRB and Saad AH. *Gravity and Magnetic Exploration*, Cambridge University Press, Cambridge, 2013; 525 p.
- [28] Luo Y, Xue D, Wang M. Reduction to the pole at the equator. *Chinese Journal of Geophysics*, 53, 2010; pp. 1082-1089
- [29] Gun PJ. Linear transformation of gravity and magnetic fields. *Geophysical Prospecting*, 1975; 23, pp. 300-312.
- [30] Miller HG and Singh V. Potential field tilt - A new concept for location of potential field sources. *Journal of Applied Geophysics*, 1994; 32: 213-217
- [31] Nabighian, M.N. 1974. Addition comment on the analytic signal of two dimensional bodies with polygonal cross section-its properties and use for automated anomaly interpretation. *Geophysics*, 39: 85-92.
- [32] Roest, W. R. and Pilkington, M. Identifying remanent magnetization effects in magnetic data. *Geophysics*, 58 (5): 653 - 659 (1993).
- [33] Phillips JD. Potential field geophysical software for P.C version 2.2. Open file report 97 725, 1997
- [34] Blakely RJ and Simpson RW. Approximating edges of sources bodies from magnetic or gravity anomalies. *Geophysics*, 1986; 51(7): 1494 - 1498.
- [35] Fairhead JD, Green CM., Verduzco B and MacKenzie C. A new set of magnetic field derivatives for mapping minerals prospects. ASEG 17th Geophysics Conference and Exhibition, Sydney, Extended Abstract, 2004
- [36] Blakely RJ. *Potential theory in gravity and magnetic applications*: Cambridge University Press, 1996.
- [37] Verduzco B, Fairhead JD, Green CM. and MacKenzie C. New insights into magnetic derivatives for structural mapping: *The Leading Edge*, 2004, 23: 116-119.
- [38] Baranov V. A new method for interpretation of aeromagnetic maps using Pseudo- gravimetric anomalies. *Geophysics*, 1957; 22: 359 - 38.
- [39] Holden E, Dentith M and Kovesi P. Towards the Automatic Analysis of Regional Aeromagnetic Data to Identify Regions Prospective for Gold Deposits. *Computers and Geosciences*, 2008;34(11): 1505 - 1513.
- [40] Holden E, Kovesi P, Dentith M, Wedge D, Wong JC. and Fu SC. Detection of Regions of Structural Complexity within Aeromagnetic Data Using Image Analysis. Twenty Fifth International Conference of Image and Vision Computing, New Zealand, 2010.
- [41] Holden EJ, Fu SC, Kovesi P, Dentith M, Bourne B and Hope M. Automatic Identification of Responses from Porphyry Intrusive Systems within Magnetic Data Using Image Analysis. *Journal of Applied Geophysics*, 2011; 74: 255 - 262.
- [42] Core D, Buckingham A, Belfield S. Detailed structural analysis of magnetic data —done quickly and objectively. *SGEG Newsletter*, 2009.

- [43] Dentith M. Texture analysis of aeromagnetic data. Proceedings Australian Society of Exploration Geophysicists (ASEG) 2000 Aeromagnetism — State of the Art Enhancement Workshop. Cowan Geodata Services, 2000. pp. 115–128.
- [44] Macnae J. Applications of geophysics for the detection and exploration of kimberlites and lamproites. In: Griffin WL (Ed.), Diamond Exploration into the 21st Century. Journal of Geochemical Exploration, 1995; pp. 213–243
- [45] Feumoe S, Ndougsa-Mbarga T, and Manguelle-Dicoum. Delineation of tectonic lineaments using aeromagnetic data for the south-east Cameroon area. Geofizika, 2012; 29: 175-192

To whom correspondence should be addressed: Dr. Olurin Oluwaseun Tolutope, Department of Physics, Federal University of Agriculture Abeokuta, Nigeria E-mail: olurin@physics.unaab.edu.ng